Analysis of Sulfur Biochemistry of Sulfur Bacteria Using X-ray Absorption Spectroscopy†

Ingrid J. Pickering,*,‡ Graham N. George,*,‡ Eileen Y. Yu,‡ Daniel C. Brune,§ Christian Tuschak,||,⊥ Jörg Overmann,||,⊥ J. Thomas Beatty,|| and Roger C. Prince*,#

Stanford Synchrotron Radiation Laboratory, Stanford Linear Accelerator Center, MS 69, 2575 Sand Hill Road, Menlo Park, California 94025, Department of Chemistry, Arizona State University, Tempe, Arizona 85287, Department of Microbiology and Immunology, University of British Columbia, Vancouver, British Columbia, V6T 1Z3, Canada, and ExxonMobil Research and Engineering Company, Route 22 East, Annandale, New Jersey 08801

Received March 19, 2001; Revised Manuscript Received May 4, 2001

ABSTRACT: Many sulfide-oxidizing organisms, including the photosynthetic sulfur bacteria, store sulfur in "sulfur globules" that are readily detected microscopically. The chemical form of sulfur in these globules is currently the focus of a debate, because they have been described as "liquid" by some observers, although no known allotrope of sulfur is liquid at physiological temperatures. In the present work we have used sulfur K-edge X-ray absorption spectroscopy to identify and quantify the chemical forms of sulfur in a variety of bacterial cells, including photosynthetic sulfur bacteria. We have also taken advantage of X-ray fluorescence self-absorption to derive estimates of the size and density of the sulfur globules in photosynthetic bacteria. We find that the form of sulfur that most resembles the globule sulfur is simply solid S_8, rather than more exotic forms previously proposed.

Sulfur is essential for all life, but it plays a particularly central role in the metabolism of many anaerobic microorganisms. Sulfate acts as electron acceptor for the sulfate-reducing bacteria, while sulfide and sulfur can act as electron donor in many photosynthetic and chemoautotrophic bacteria. As discussed as early as 1887 by Winogradsky for the case of *Beggiatoa* (*1*), many sulfide-oxidizing organisms, including the photosynthetic sulfur bacteria, store sulfur in "sulfur globules" that are readily detected microscopically (*2*, *3*). These globules are found within (e.g., in the Chromatiaceae and Beggiatoaceae) or outside (e.g., the Chlorobiaceae) the cell wall, although in both cases they are extracellular in that they are external to the cytoplasm. Sulfur globules can be quite large, up to a micrometer in diameter, and at least some are surrounded by a layer of protein (*4*). Studies using polarizing microscopy and X-ray diffraction (*5*) have been used to argue that the globules contain sulfur in a liquid form, a surprising conclusion as no known allotropes of elemental sulfur are liquids at physiological temperatures. The globules also exhibit several properties that would not be expected of elemental sulfur; in particular they are hydrophilic, and have relatively low apparent densities. On the other hand, like some sulfur allotropes, they are (at least partly) soluble in carbon disulfide and other organic solvents (see ref *3* and refs therein). Several hypotheses have been developed to explain these apparent discrepancies. Steudel (*3*) has suggested that the sulfur globules are vesicles formed of a monolayer of long-chain polythionates [$S_m(SO_3)_2^{2-}$] enclosing a water-filled cavity, which may itself contain other polythionate micelles. More recent work, using sulfur K-edge X-ray absorption spectroscopy (*6*), has been interpreted as evidence for long chains of sulfur terminated by carbon atoms.

The near-edge region of the X-ray absorption spectrum is dominated by dipole-allowed ($\Delta l = \pm 1$) bound-state transitions of the 1s electron (for a K-edge) to vacant molecular orbitals with substantial p-character. The near-edge spectrum thus provides a sensitive probe of electronic structure and hence of chemical form. Sulfur exhibits particularly rich K near-edge spectra due to relatively sharp line widths and large chemical shift range and is thus a very useful tool for speciating sulfur in complex biological samples (*7*), although it must be used with care to ensure that artifacts are not introduced into the data. We have taken advantage of some of the limitations we have discussed before, such as the small penetration depth of photons of these energies, to derive equations to determine the size and density of the sulfur globules in photosynthetic bacteria. We followed the formation and disappearance of globules in a laboratory culture, but found no evidence for anything other than solid S_8 in the globules. We discuss the potential limitations of this conclusion and the experimental flaws in previous work (*6*) that, we contend, led to erroneous conclusions.

* To whom correspondence should be addressed. Phone: (650) 926-4604. Fax: (650) 926-4100. E-mail: george@ssrl.slac.stanford.edu.

† This work was supported in part by the National Institutes of Health GM57375 and the NSERC. The Stanford Synchrotron Radiation Laboratory is funded by the Department of Energy, Offices of Basic Energy Sciences and Biological and Environmental Research; the National Institutes of Health, National Center for Research Resources, Biomedical Technology Program, and the National Institute of General Medical Sciences.

‡ Stanford Synchrotron Radiation Laboratory.

§ Department of Chemistry, Arizona State University.

|| Department of Microbiology and Immunology, University of British Columbia.

⊥ Present address: Institut für Genetik und Mikrobiologie, Universität München, Maria-Ward Strasse 1a, D-80638 München, Germany.

ExxonMobil Research and Engineering Company.

10.1021/bi0105532 CCC: $20.00
Published on Web 06/07/2001

MATERIALS AND METHODS

Growth and Preparation of Bacteria. Allochromatium vinosum and *Amoebobacter purpureus* (both members of the Chromatiaceae) and *Chlorobium tepidum* (a member of the Chlorobiaceae) were cultivated photoautotrophically with sulfide as electron donor (*8*). *Chloroflexus aurantiacus* (a member of the Chloroflexaceae) and *Heliobacterium chlorum* (a member of the Heliobacteriaceae) were cultivated photoheterotrophically on yeast extract (*9*), while *Al. vinosum* was additionally cultivated photoheterotrophically on malate as previously described (*10*), but omitting yeast extract and vitamin B12 (not required by *Al. vinosum*) and at pH to 7.5 (the same pH that was used for the autotrophic medium). *Rhodobacter capsulatus* (a member of the Rhodobacteriaceae) was cultivated both photoheterotrophically and aerobically on malate (*11*). Natural samples of a marine *Beggiatoa* were collected from the Guaymas hydrothermal vent site (*12*), and *A. purpureus* was collected from Mahoney Lake (*13*). Sulfur globules were prepared from photoautotrophically grown *Al. vinosum* as previously described (*8*).

X-ray Absorption Spectroscopy. Sulfur K-edge X-ray absorption spectroscopy was carried out on beam line 6-2 of the Stanford Synchrotron Radiation Laboratory essentially as previously described (*7*), using the program XAS Collect for data acquisition (*14*). Crystals of α-S_8 were intimately ground with graphite to minimize charging artifacts. The powder was mounted on Mylar adhesive tape, and its spectrum measured using total electron yield; all other standard compounds (Figure 1) were measured as buffered aqueous solutions at room temperature by monitoring X-ray fluorescence. Bacteria were prepared as dilute suspensions of cultures in cuvettes with 6.3 μm polypropylene windows. Bacterial samples were frozen in liquid nitrogen and then maintained at a temperature of −20 °C during data acquisition (except for *C. tepidum*, which was run at room temperature). X-ray absorption spectra were measured by monitoring the X-ray fluorescence using a Stern-Heald-Lytle fluorescent ion chamber detector (EXAFS Company, Pioche, NV) mounted at 90° to the incident beam. The X-ray energy was calibrated with reference to the lowest energy peak of sodium thiosulfate ($Na_2S_2O_3 \cdot 5H_2O$), which was assumed to be 2469.2 eV (*15*).

Calculation of X-ray Absorption from Spheres. Fluorescence is ideally proportional to the absorption coefficient only for samples that are dilute or thin. When this is not the case, the deviations from proportionality are called thickness effects or, more commonly, self-absorption. Previous calculations involving self-absorption effects (see ref *16* and refs therein) have focused on extracting a distortion-free spectrum from an observed spectrum which is distorted in a quantifiable way, for example in the case of a sample which is infinitely thick with respect to the penetration depth of the incident photon. Here we take a different approach, as we use the self-absorption effect to derive metrical details (radius and density) of the particles in addition to the identity of the phase and its fractional contribution to the total sulfur present.

The fluorescence from a sphere is calculated by dividing the sphere into small volume elements, considering the contribution of a generic volume element to the total fluorescence, then numerically integrating over all volume elements. It is assumed that the sphere is illuminated using a beam of constant intensity, and the simplification is made that the detector collects the fluorescence at 90° to the incident beam.

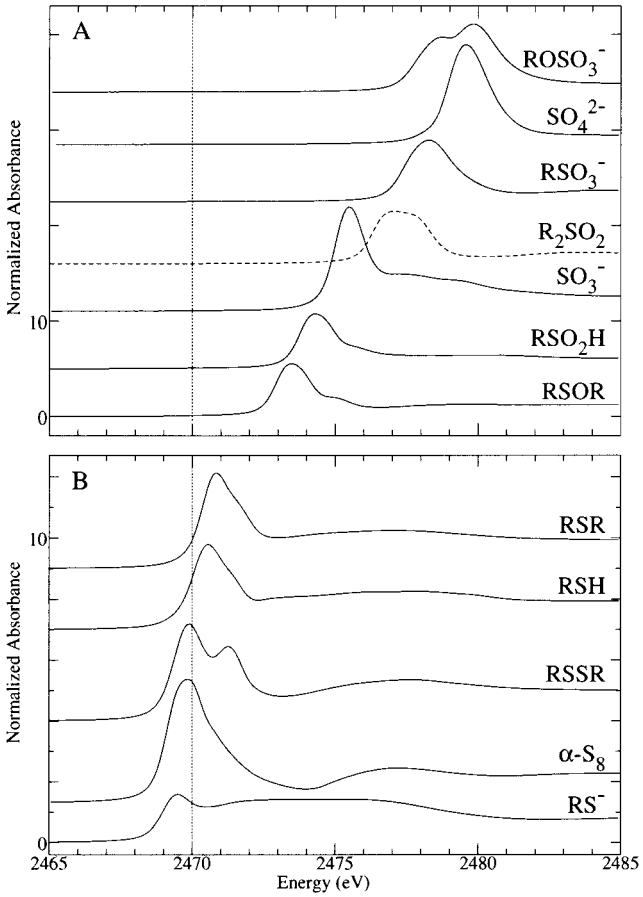

FIGURE 1: Sulfur K X-ray absorption near-edge spectra of the standard compounds which were tested in the fits. Unless otherwise stated, spectra were collected using fluorescence on 50−100 mM (in sulfur) aqueous solutions, buffered in bicine at pH 7. Top to bottom: $ROSO_3^-$, sodium methyl sulfate; SO_4^{2-}, potassium sulfate (pH 8); RSO_3^-, cysteic acid; R_2SO_2, dimethyl sulfone (pH 8); SO_3^-, sodium sulfite (not buffered); RSO_2H, cysteinesulfinic acid; RSOR, DL-methionine sulfoxide; RSR, methionine; RSH, reduced glutathione; RSSR, oxidized glutathione; α-S_8 (powder mixed with graphite, measured in electron yield); RS^-, cysteine (pH 13).

Consider the contribution of a volume element of dimensions *dz* (vertically), *dy* (across the beam, parallel with the path to the fluorescence detector), and *dx* (parallel with the incident beam) (Figure 2). The contribution of the volume element to the total fluorescent intensity will depend on the incident intensity, the incident beam attenuation, the fluorescence yield of the volume element, and the fluorescent beam attenuation. The intensity incident on a volume element is proportional to $I_0^{\text{unit}} e^{-\rho\sigma_E t_{in}}$, where I_0^{unit} is the incident intensity per unit area and the exponential term is the attenuation of the incident beam due to the path, t_{in}, through the sphere to that volume element. Here, ρ is the sphere density and σ_E is the absorption cross-section of the sphere material at the energy of the incident beam. σ_E is obtained by measuring the undistorted absorption spectrum of the species of interest (in our case, α-S_8 mixed with graphite measured in electron yield) and scaling this spectrum to the theoretical absorption cross-section (*17*). The fluorescence generated by the volume element per unit incident intensity

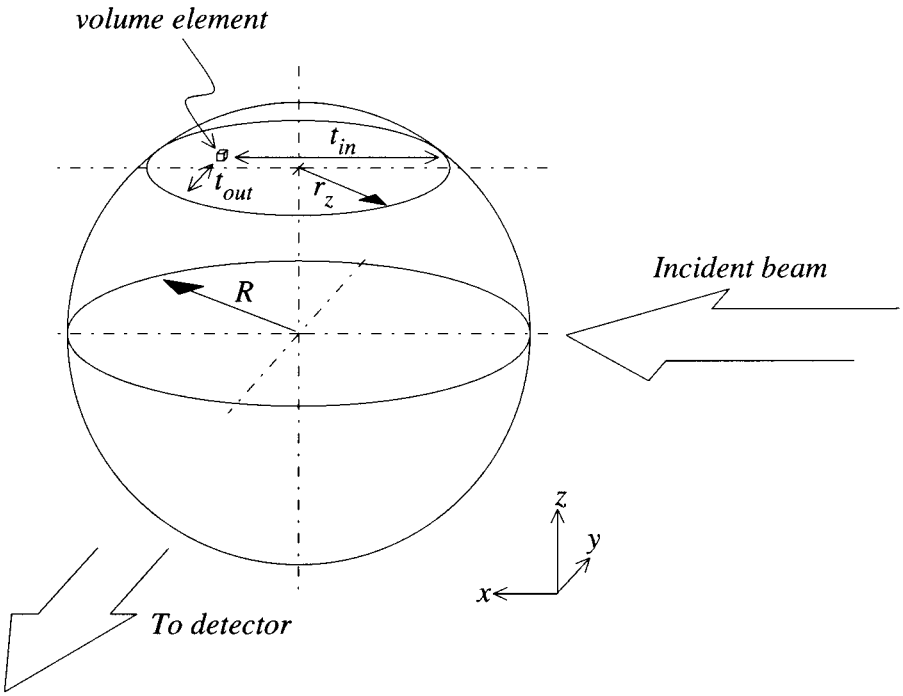

FIGURE 2: Coordinate system used for calculation of sulfur K near-edge spectra of spheres.

is proportional to its absorbance and can be written as $\epsilon\rho\sigma_E$ dx, where ϵ is a constant (proportional to the fluorescence efficiency). Finally, the attenuation of the outgoing fluorescence photons is proportional to $e^{-\rho\sigma_F t_{out}}$, where t_{out} is the outgoing path and σ_F is the absorption cross-section of the sphere material at the energy of the fluorescence. Hence, the total fluorescence intensity from the entire sphere of radius R may be given by

$$I_f^{sphere} \propto 2I_0^{unit}\epsilon\rho\sigma_E \int_{z=0}^{R}\int_{y=-r_z}^{r_z}\int_{x=-x_m}^{x_m} \times e^{-\rho\sigma_E t_{in}}\, e^{-\rho\sigma_F t_{out}}\, dx\, dy\, dz \quad (1)$$

Here, $r_z = \sqrt{R^2 - z^2}$ is the effective radius of a slice made with a horizontal cut, and $x_m = \sqrt{r_z^2 - y^2}$ is half the depth of the slice at horizontal point y. The paths in and out are given by $t_{in} = \sqrt{r_z^2 - y^2}$ and $t_{out} = \sqrt{r_z^2 - x^2} + y$. The total incident intensity illuminating the sphere is $I_0^{sphere} \propto \pi R^2 I_0^{unit}$, and the effective distortion-free fluorescence intensity can be expressed as $I_f^{nondist} \propto {}^4/_3\pi R^3 I_0^{unit}\epsilon\rho\sigma_E$.

To appropriately calculate the transmittance of a monolayer of close-packed spheres, both the spheres themselves and the interstitial space must be taken into account. The intensity transmitted through a single sphere, I_t^{sphere}, is calculated by considering columns of volume elements in the x direction. For such a column at position (y, z), the length of the column in the x direction is given by $d = 2\sqrt{r_z^2 - y^2}$ and hence:

$$I_t^{sphere} \propto 2I_0^{unit} \int_{z=0}^{R}\int_{y=-r_z}^{rz} e^{-\rho\sigma_E d}\, dy\, dz \quad (2)$$

The unit area occupied by a single close-packed sphere and its associated interstices can be shown to be $2\sqrt{3}R^2$, whereas the area of the single sphere is πR^2. Hence, calculated incident and transmitted intensities for the close-packed layer expressed per sphere are $I_0^{layer} = I_0^{sphere} 2\sqrt{3}/\pi$ and $I_t^{layer} = I_t^{sphere} + I_0^{sphere}[(2\sqrt{3}/\pi) - 1]$, respectively. Finally, the observed fluorescence, $F = I_f^{sphere}/I_0^{layer}$, and the observed transmittance, $T = \log_e(I_0^{layer}/I_t^{layer})$, are calculated as usual.

Figure 3 shows the calculated spectra of a monolayer of spheres of α-S_8 with varying radii for fluorescence (Figure 3A), for transmittance of a close-packed layer (Figure 3B) and for transmittance of more widely spaced spheres (Figure 3C). We note in passing that our model is not completely rigorous, as we neglect the effects of shadowing. However, it would be readily extended to model different particle morphologies, or to model particles having a depth-dependent density.

Fitting of Spectra. Data were analyzed using the EXAFSPAK suite of computer programs (*18*). Spectra of bacterial samples were deconvoluted by least-squares fitting of the data to linear combinations of the spectra of standard compounds, as previously described (*19*, *7*). Standard compounds were chosen to be representative of the functional groups of sulfur that are likely to be present. Hence, for example, the use of reduced glutathione in a fit does not necessarily give a quantitation for this particular compound, but rather for reduced, aqueous aliphatic thiols in general. A general method of fitting proceeded as follows. The spectra were fitted to the entire suite of candidate standard spectra (see Figure 1), using independent fits for both the spectra and second derivatives. The level of individual standard compounds were judged as significant if their contribution to a particular fit was at least 0.5%, and exceeded their estimated standard deviation (calculated from the diagonal elements of the variance-covariance matrix) by at least 3-fold. Only those standards which were significant in *both* the edge and the derivative fits of a particular sample were retained, the fits to the edge were repeated with this reduced basis set

[1] In the exponential terms of eqs 1 and 2, distance and density terms appear as products. Hence, we cannot determine independent values for both density and radius.

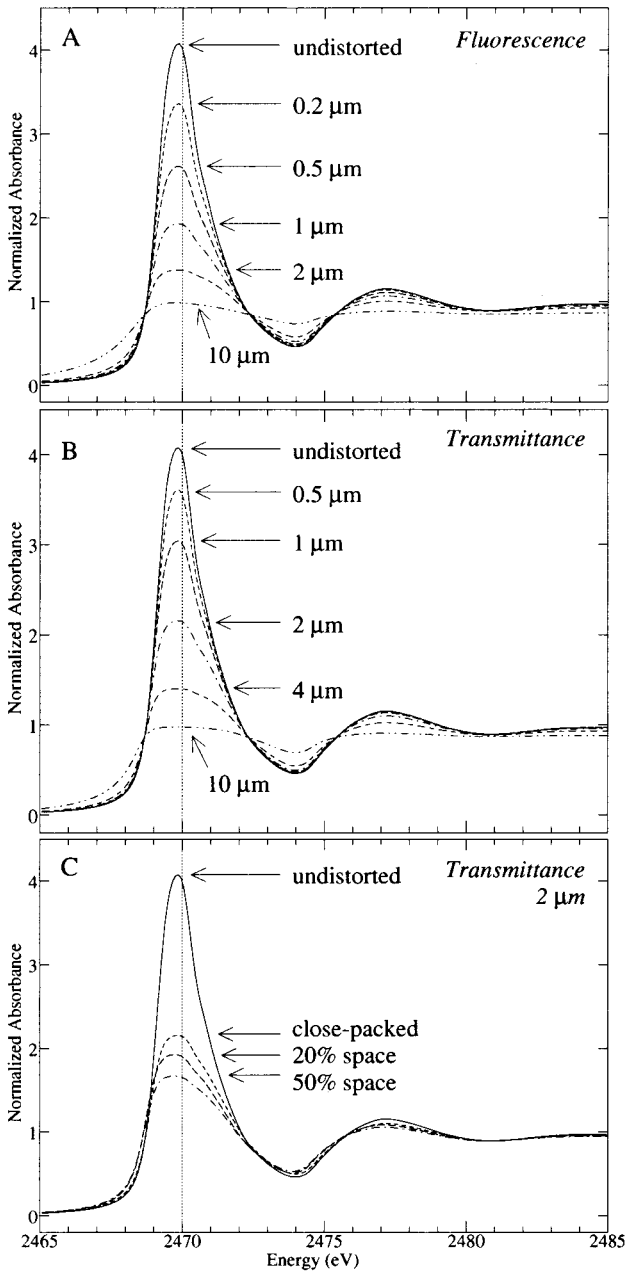

FIGURE 3: Sulfur K near-edge spectra calculated for spheres of α-S_8. We show the spectra calculated for a single layer of spherical particles of various radii for (A) fluorescence, (B) transmittance of a close-packed monolayer, and (C) transmittance of a monolayer of 2 μm radius spheres with varying proportions of space introduced. In each case, the "undistorted" spectrum is measured in electron yield from a powder mixed with graphite, and the calculations assume the observed density of bulk α-S_8 (2.069 g cm^{-3}). If the true density of the spheres is different to this, then the radius for a given calculated spectrum will scale accordingly.[1]

and the same significance criteria applied. In cases where spherical sulfur particles were found to be significant, individual fits of the edge data were carried out using the spectra representing each particle size and the fit residuals were used to determine which size gave the best fit. The significance criteria described above were then used to reject components from the fit employing the optimum particle size, and then the size dependence was reevaluated using the reduced set of spectra.

In principle, the fitting procedure can also give absolute concentrations of sulfur. In the present case, samples were

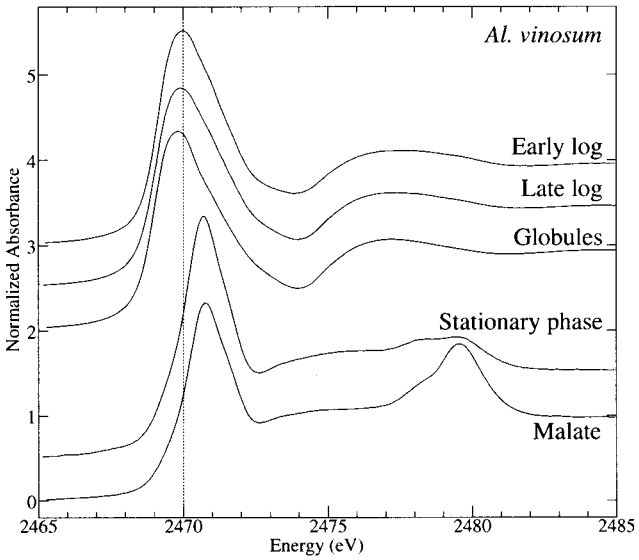

FIGURE 4: Sulfur K near-edge spectra from *Al. vinosum* cultured under various conditions. Top to bottom, early log phase, late log phase, globules (extracted from the late log phase), and the stationary phase from *Al. vinosum* cultured photoautotrophically, and *Al. vinosum* cultivated photoheterotrophically on malate.

suspensions of bacterial cultures (rather than packed cells), so that absolute concentrations of sulfur are difficult to relate to cellular levels.

Although the precisions (estimated standard deviations) are simple to calculate, estimates of the accuracies are more difficult to obtain, as these will depend on the degree of similarity between the standard spectra chosen and their counterparts in the composite spectrum which is being fitted. Similarly, the accuracies for estimates of the radius and density of particles[1] depend critically on the approximations inherent in our analysis (e.g., homogeneous spherical particles). Thus, we expect accuracies to be somewhat larger than the precisions and to vary on a case-by-case basis.

The use of calculated spectra for spherical morphology requires an adjustment to the results of the deconvolution because the sulfur present as spherical material will be underrepresented since the spheres themselves attenuate the beam much more than the medium. To correct this, spectra are computed using both I_f^{sphere} and $I_f^{nondist}$, and both these computed spectra are normalized to give the respective normalization constants C_{sphere} and $C_{nondist}$. The apparent fraction of the sphere material present in the mixture then needs to be augmented by $C_{nondist}/C_{sphere}$. In general, this correction factor increases with increasing radius, and has the values of 1.17 and 1.41 for radii of 0.40 and 0.90 μm, respectively. After application of the correction factor, the relative sulfur contents are renormalized to obtain the percentage contributions.

RESULTS

Figures 4−6 show the sulfur K-edge X-ray absorption spectra of several photosynthetic and nonphotosynthetic bacterial samples. *Al. vinosum* is a typical example of the Chromatiaceae, the purple-sulfur bacteria, and its sulfur globules have been extensively studied (*2*, *3*). *Al. vinosum* also has the ability to grow heterotrophically on malate in the absence of sulfide, allowing us to use cells grown in this way as a control. Figure 4 shows the spectra of cells at

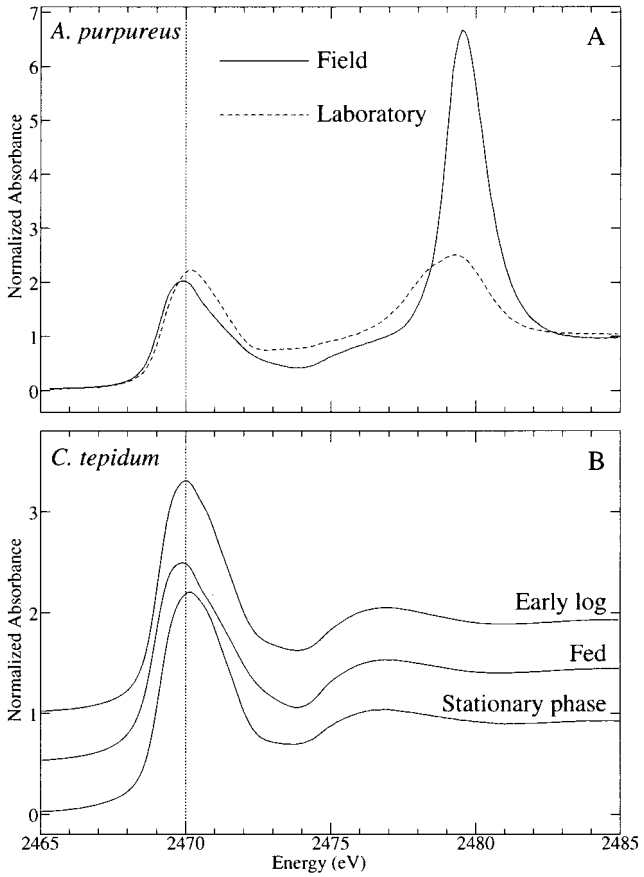

FIGURE 5: Sulfur K near-edge spectra: (A) *A. purpureus* collected from Mahoney lake (field) and cultivated photoautotrophically to late log phase (laboratory); (B) early log phase, fed, and stationary phases of *C. tepidum* cultivated photoautotrophically. Fed cultures received additional aliquots of sulfide during growth; only low levels are tolerated by dilute cultures.

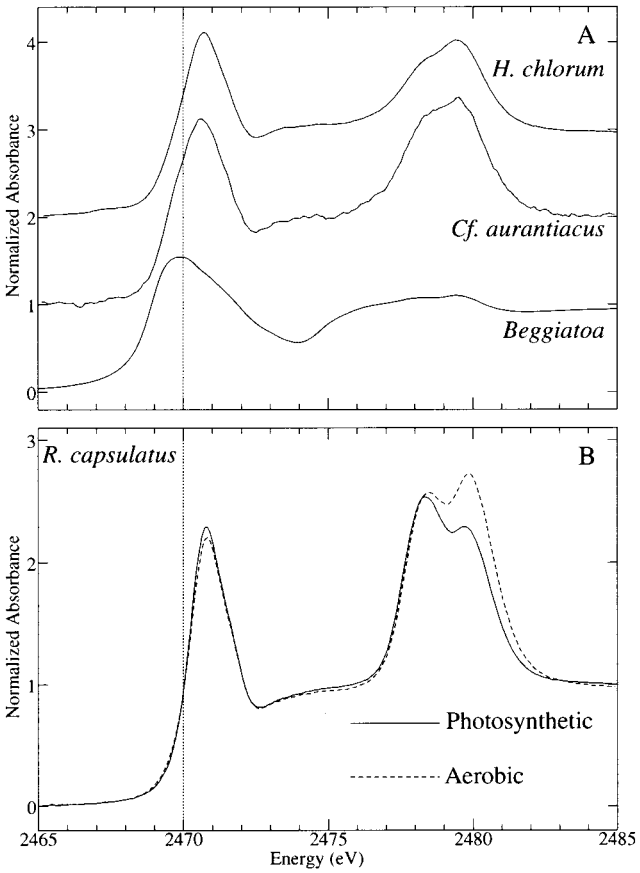

FIGURE 6: Sulfur K near-edge spectra: (A) *H. chlorum* and *Cf. aurantiacus* grown photoheterotrophically on yeast extract, and marine *Beggiatoa* collected from the Guaymas hydrothermal vent site (*12*); (B) *R. capsulatus* grown photoheterotrophically and aerobically on malate.

three different stages of photoautotrophic growth, together with the spectrum of isolated sulfur globules, and the spectrum of cells grown photoheterotrophically on malate in the absence of sulfide. As expected, the photoautotrophic cells seem to have a substantial contribution from the sulfur globules, while the photoheterotrophic cells do not.

Figure 5 presents spectra of *A. purpureus*, another member of the Chromatiaceae, both grown in the laboratory to late log phase, and collected from Mahoney Lake in British Columbia, Canada. This lake has a very dense layer of these bacteria growing at the anoxic/oxic interface, representing the densest population of photosynthetic bacteria found in the environment to date (*13*). The figure also presents spectra of a laboratory culture of *Chlorobium tepidum*, a member of the Chlorobiaceae (green sulfur bacteria). As expected, the spectra from both organisms suggest a significant amount of sulfur globules, which are known to reside inside the cell in the former, and outside in the latter organism. Figure 6 presents spectra of three other photosynthetic bacteria, from the three other known families; *Heliobacterium chlorum*, a member of the green non-sulfur bacteria (Heliobacteriaceae), *Chloroflexus aurantiacus*, a member of the green gliding bacteria (Chloroflexaceae), and *Rhodobacter capsulatus*, a member of the purple non-sulfur bacteria (Rhodospirillaceae). All of these cultures were grown in the absence of sulfide and, as expected, the samples lacked sulfur globules. The figure also shows the spectrum of a natural sample collected from the Guaymas hydrothermal vent site (*12*) in which a marine *Beggiatoa sp.* was predominant. This organism is nonphotosynthetic, and grows autotropically with sulfide as electron donor and oxygen as terminal electron acceptor. As expected from Winogradsky's early work (*1*), the *Beggiatoa* sample has a substantial amount of sulfur globules.

We have previously shown that it is possible to quantitatively analyze the sulfur-containing species in biological systems by least squares-fitting to the sum of spectra of potential standard compounds (*7*). Figure 1 shows the spectra of some sulfur-containing species that are potentially present in these bacteria. The presence of a locally very concentrated form of sulfur in the sulfur globules lends the additional complication that the X-ray fluorescence is no longer directly proportional to concentration, and this in turn leads to apparent distortions of the spectra. Because the issue is one of *local* concentration, it cannot be overcome by simply diluting the sample. Fortunately, the phenomenon can be quantified, and we have taken advantage of it to estimate the size and density of the sulfur globules in the bacterial samples, as well as their composition and relative abundance.

To start the analysis of this phenomenon, which is discussed in detail in the Materials and Methods, the undistorted spectra of candidate standard compounds are required. For most compounds these are available from measurements of appropriately dilute solutions, but for α-S_8 undistorted data can be readily obtained only by using total electron yield measurements. Because the electron path

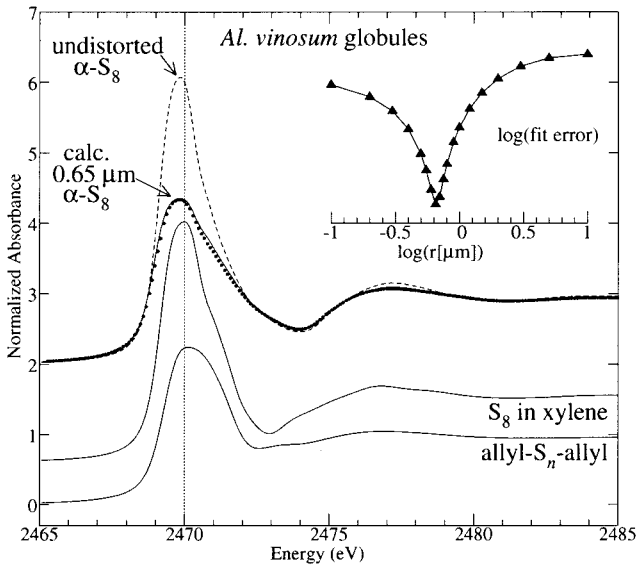

FIGURE 7: Sulfur K near-edge spectra from globules extracted from *Al. vinosum* late log phase (filled circles) in comparison with spectra of α-S_8, S_8 dissolved in xylene, and allyl polysulfides. The α-S_8 spectrum is shown both undistorted, and as calculated for 0.65 μm radius spheres (with density of 2.069 g cm^{-3})[1] measured in fluorescence, which gave the best fit to the experimental data. The inset shows a log plot of the residual as a function of the calculated radius, and exhibits a sharp minimum.

length is tiny in comparison to that of the photon, electron yield measurements are essentially impervious to artifacts related to high sample concentrations. Using the undistorted spectrum of α-S_8 thus obtained, and assuming a spherical particle, we consider a small volume element of that sphere. We calculate the attenuation by the sphere both of the incident beam in penetrating to that volume element and of the outgoing fluorescent beam in the direction of the detector. We then numerically integrate over the entire sphere to obtain the total spectrum, distorted due to the specific radius of the particle. We calculate spectra for a suite of different radii, use them in individual fits of the spectra from bacteria, and monitor the fit-error as a function of radius (see inset to Figure 7) to choose the optimal radius for that spectrum.

Figure 7 shows the best fit to the sulfur globules extracted from *Al. vinosum*; the radius determined by this method is 0.65 μm (assuming the density of α-S_8)[1] which is in agreement with microscopic examination. It is clear from this figure that the correspondence between the 0.65 μm radius spectrum of α-S_8 and the spectrum of the globules is excellent. In particular, the structure on the high energy side of the absorption threshold, typically an indicator of differences in next-nearest or more distant atoms, is essentially identical, indicating that solid S_8 with spherical morphology is an excellent model for the sulfur in the globules. In contrast, the spectra of S_8 in xylene and allyl-S_n-allyl are rather different in this postedge region, with their minima occurring at quite different energies.[2]

Because the globules in the bacterial samples are unlikely to be of completely uniform size, we have investigated possible effects arising from this by computing near-edge spectra using a distribution in particle sizes. A computer program was written which numerically integrated spectra over a Gaussian distribution either of particle radii *R*, of surface areas, or of particle volumes (masses). The resulting spectra were only slightly different from the spectrum computed for a single particle at the mean radius. For a distribution in *R*, the effect was that the computed spectra resembled those of particles of slightly larger radius than the mean, while for volume and area more subtle effects were observed, and resembled spectra of particles of very slightly smaller radii. Thus, using a mean particle radius of 0.65 μm with the density of α-S_8, and with a Gaussian distribution in *R* of half-width 0.33 μm, the computed spectrum was essentially identical to that computed for a single particle of radius 0.70 μm (not illustrated). We conclude that the spectra are relatively insensitive to distributions in particle sizes, and that any errors resulting from neglect of this in our analysis will be small.

Table 1 summarizes the results of fitting of the near-edge spectra of the various bacterial samples, and Figure 8 shows examples of the breakdown of two of the fits. Figure 8A shows an example of a fit in which the bulk of the sulfur is elemental sulfur,[3] while Figure 8B shows a more complex fit in which other sulfur forms predominate. From the table it can be seen that both the size of sulfur globules and the proportion of total sulfur present as this form increase between the early and late log phases of *Al. vinosum*, and then decrease in the stationary phase. A similar trend is seen for *C. tepidum*.

DISCUSSION

Many, but by no means all, photosynthetic (e.g., *Al. vinosum*, *A. purpureus*, *C. tepidum*) and nonphotosynthetic (e.g., *Beggiatoa*) bacteria that oxidize sulfide are able to transiently store reductant as elemental sulfur until sulfide levels drop, when they apparently oxidize the stored sulfur to sulfate. In all cases known, the sulfur globules are external to the cell cytoplasm; in some cases they are periplasmic, while in others they are outside the cell wall. Just how organisms that "store" sulfur globules outside the cell wall access this source of reductant remains an open question, but at least in pure culture it is clear that this sulfur reservoir is used when sulfide levels are low.

From our model (elaborated above), we seek to derive estimates of various unknowns: the density and radius of the particle; the chemical nature of the phase; and the fraction of total sulfur present in the particles. In calculating the spectra for various radii we initially assumed the density of 1.31 g cm^{-3} estimated by Guerrero et al. (*20*). However, this led to estimated radii for the globules which were clearly much too large (i.e., $\sim$2 μm). Alternatively, employing the density of α-S_8 [2.069 g cm^{-3} (*21*)] yielded radii that were commensurate with the results of microscopic examination (see refs *2*, *3*, and *8*). Previous estimates of the density of the globules were calculated from flotation measurements

[2] The spectrum of γ-S_8 (prepared by rapid crystallization from boiling hexane) was also collected in electron yield (data not shown). In this case, the powder was not ground with graphite as grinding might cause reversion to the stable allotrope α-S_8. For this reason the spectra are subtly distorted due to charging effects, but it is clear that the absorption maxima and minima are at similar energies to those of α-S_8. Therefore, we cannot distinguish between these two solid forms of S_8.

[3] If the undistorted spectrum of α-S_8 is used, the resulting residual is very much worse (by more than 1 order of magnitude), the S^0 contribution is under-estimated and is compensated by changes in other components.

Table 1: Results of Curve-Fitting Sulfur K-Edge X-ray Absorption Spectra of Bacterial Cells to the Sums of Standard Spectra[a]

bacterium	sample	RSSR	RSH	RSR	R_2SO	RSO_2^-	RSO_3^-	SO_4^{2-}	α-S_8	best α-S_8 size[b] (μm)	residual[c] ($\times 10^{-2}$)
Al. vinosum	early log	8 (2)	17 (1)					0.7 (0.2)	74 (2)	0.40 ± 0.05	0.030
	late log	6 (1)	9 (1)					0.5 (0.1)	84 (1)	0.60 ± 0.05	0.014
	stationary phase		41 (5)	40 (4)	3 (1)		1 (1)	2 (1)	13 (1)	<0.01	0.098
	malate	13 (2)	31 (4)	42 (3)	3 (1)		3 (1)	8 (3)			0.073
	globules							0.4 (0.1)	99.6 (0.3)	0.65±.05	0.021
A. purpureus	field							45 (1)	55 (2)	0.3 ± 0.1	1.699
	laboratory	23 (7)	31 (4)				14 (1)	11 (1)	20 (4)	<0.01	0.322
C. tepidum	early log		10 (3)	6 (2)		2 (0.3)			82 (1)	0.45 ± 0.05	0.052
	fed		2 (1)			1 (0.3)			97 (1)	0.90 ± 0.05	0.028
	stationary phase	4 (3)	17 (4)	6 (3)		2 (0.5)			71 (3)	0.50 ± 0.05	0.075
Cf. aurantiacus	late log	24 (4)	54 (4)				12 (1)	10 (7)			0.489
H. chlorum	late log	19 (2)	35 (5)	24 (3)	5 (1)		9 (1)	8 (1)			0.113
R. capsulatus	photosynthetic		25 (3)	49 (3)			11 (1)	15 (1)[d]			0.096
	aerobic		22 (5)	49 (5)			5 (1)	24 (1)[d]			0.279
Beggiatoa	field			0.8 (0.9)			0.6 (0.3)	1.0 (0.2)	97.5 (1)	1.6 ± 0.1	0.051

[a] Percentage contributions of sulfur species to total sulfur inventory. Key for standard spectra as for Figure 1. The spectra of RS^-, R_2SO_2, and SO_3^- were also tested, but were excluded from all fits. Value in parentheses shows the 95% confidence limit (obtained from the diagonal element of the covariance matrix) in the last digit(s) of the percentage. We note that when components are not determined, this does not necessarily indicate their absence in the sample. As discussed in the materials and methods section components were excluded at levels less than 0.5% or above three times their estimated standard deviation. [b] Assumes a density of 2.069 g cm^{-3}.[1] [c] Residual is the average of the sum of the squares of the differences between the observed and calculated signals for all data points in the spectrum. [d] Values are for sulfate ester ($ROSO_3^-$) which gave a substantially better fit than did sulfate (SO_4^{2-}). When both were included in the fit, sulfate was rejected.

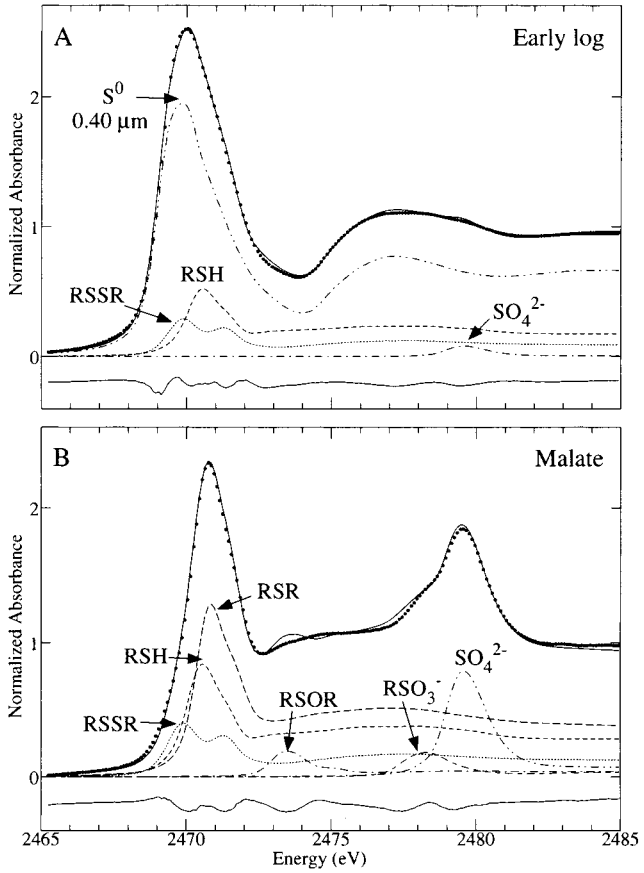

FIGURE 8: Results of fitting the S K near-edge spectra of (A) photoautotrophic early log and (B) photoheterotrophic cultures of *Al. vinosum*. The data are shown as filled circles, the best fit as the solid line, and the residual as the solid line beneath the data. The constituent spectra used for the fit are shown as various dashed and dotted lines, scaled according to their proportions in the fit (see Table 1), and labeled as for Figure 1.

of whole cells (*20*), and our results indicate that these estimates must be erroneously low. In addition, our observations that the observed spectrum of sulfur globules is extremely similar to that of solid S_8 with spherical morphology, and unlike other closely related species, suggests that the true phase of sulfur in the globules is simply solid S_8.

Thus, the spectrum of the globules provides no support for the hypothesis that the sulfur chains are terminated by carbon moieties. Although samples of long-chain polythionates were unavailable to us, the bulk of the sulfur in these compounds is in S_n linear chains and should resemble polysulfides. To achieve an adequate match to the globules fit, both minima and maxima of the spectra would need to be in the same place as those of S_8. It its extremely unlikely that their spectra would closely resemble that of α-S_8, and we believe that this hypothesis can also now be discounted.

The sequences of the proteins surrounding the sulfur globules have been reported (*8*, *4*); they contain some methionines but no cysteines or cystines. Our analyses detect none of these species (detection limit 0.5% of total S), again indicating that the vast majority of the sulfur associated with the sulfur globules is present as the elemental form. In support of this, calorimetric measurements have been carried out on an aqueous preparation of sulfur globules extracted from *Al. vinosum* (data not shown). These results indicated no phase change between +50 and −150 °C, apart from those due to the water content of the preparation. On elevating the temperature, phase transitions were observed at 106.5, 115 (small), and 121.6 °C. Measurements at higher temperatures were not done due to concerns about the tubes bursting. α-S_8 exhibits a complex phase transformation behavior to the less-dense β-S_8 and other forms at around these temperatures (*21*) and our observations are consistent with the presence of an α-S_8-like form of sulfur in the globules.

Although fluorescence is prone to distortions in more concentrated samples, transmittance measurements should in principle be distortion-free. However, to achieve this ideal requires a sample that is homogeneous, not only in its composition, but also in its thickness across the entire area the beam intersects. Unfortunately, given the optimal thickness of a film of α-S_8 (~4 μm for a maximum absorbance of 2), transmittance spectra at such low energies are

particularly susceptible to "pinhole" effects, whereby holes or thin parts in the sample transmit X-rays much more readily than the rest of the sample.

For comparison to the fluorescence case, we have modeled the transmittance for a single layer of close packed spheres. We note that in practice a real sample of a ground powder will be much less homogeneous than this ideal. Under such conditions, the spectral distortions (Figure 3B) look remarkably similar to those calculated for the fluorescence (Figure 3A), although for a given sphere radius, the transmittance is less distorted than the fluorescence. However, as more space is introduced between the particles (Figure 3C), the spectra become increasingly more distorted. It can be seen from the figure that, assuming that the powdered sample is in the form of spheres, such spheres need to be smaller than 0.2 μm for the transmittance spectrum to be essentially free of distortions. Such a small size is impossible to obtain by conventional grinding techniques.

In the case of Prange et al. (*6*), who carried out a study of the sulfur globules in *Al. vinosum*, the spectra of elemental sulfur standards were collected by measuring the transmittance of powder on tape and, we believe, were prone to the pinhole distortions described above. Indeed, the spectrum reported for α-S_8 (*6*) is very similar to the distorted spectrum calculated for 10 μm spheres shown in Figure 3. In particular, Prange et al. (*6*) based their conclusions largely on the apparent intensity of the prominent peak on top of the edge. They concluded from this that the sulfur in the globules could not be a S_n ring, but instead was a long-chain polysulfide species. We suggest that the samples of these latter compounds yielded the most intense peaks because they are oils rather than solids and are thus less prone to pinhole effects. The lower density and lower mass-fraction of sulfur in these compounds would also contribute to reducing the distortion.

In conclusion, we have used sulfur K-edge X-ray absorption spectroscopy to study the sulfur species associated with intact cells of bacteria. In particular, we have shown that the "sulfur globules" found in *Al. vinosum*, *C. tepidum*, and *Beggiatoa* samples are well-modeled by α-S_8 with spherical morphology, and have derived algorithms to quantify the size and density of these spheres. We see no evidence for a "liquid" form of sulfur, nor do we see evidence for chains of sulfur terminated by thionate or carbon-based functional groups. Our work also indicates that previous density estimates of sulfur globules are too low. However, the hydrophilic nature of the sulfur globules remains a conundrum. The near-edge spectrum is sensitive to long-range structure only up to 5−10 Å, and the presence of large-scale crystallites of α-S_8 can be excluded based on previous X-ray diffraction results (*5*). We therefore suggest a model consisting of a core of fragments with local structures resembling α-S_8, with a modified globule surface conferring hydrophilic properties. This might be due to the globule proteins, or alternatively from modification of surface sulfur atoms to incorporate a polar group such as the thionate, as previously proposed by Steudel (*3*). In either case, the surface sulfur content must constitute such a small fraction of the total as to be unobservable by our technique.

ACKNOWLEDGMENT

We are grateful to Dr. Fevzi Daldal at the University of Pennsylvania for the gift of the *R. capsulatus* cells, and to Dr. Eric Block at State University of New York at Albany for providing the sample of allyl-S_n-allyl.

REFERENCES

1. Winogradsky, S. (1887) *Botanische Zeitung 31*, 490−507.
2. Brune, D. C. (1989) *Biochim. Biophys. Acta 975*, 189−221.
3. Steudel, R. (1989) in *Autotrophic Bacteria* (Schlegel, H. G., and Bothwien, B., Eds.) pp 289−303, Springer-Verlag, Berlin.
4. Pattaragulwanit, K., Brune, D. C., Trüper, H. G., and Dahl, C. (1998) *Arch. Microbiol. 169*, 434−444.
5. Hageage, G. J., Jr., Eanes, E. D., and Gherna, R. L. (1970) *J. Bacteriol. 101*, 464−469.
6. Prange, A., Arzberger, I., Engemann, C., Modrow, H., Scumann, O., Trüper, H. G., Steudel, R., Dahl, C., and Hormes, J. (1999) *Biochim. Biophys. Acta 1428*, 446−454.
7. Pickering, I. J., Prince, R. C., Divers, T., and George, G. N. (1998) *FEBS Lett. 441*, 11−14.
8. Brune, D. C. (1995) *Arch. Microbiol. 163*, 391−399.
9. (a) Betti, J. A., Blankenship, R. E., Natarajan, L. V., Dickinson, L. C., and Fuller, R. C. (1982) *Biochim. Biophys. Acta 680*, 194−201. (b) Gest, H., and Favinger, J. L. (1983) *Arch. Microbiol. 136*, 11−16.
10. Schedel, M., Vanselow, M., and Trüper, H. G. (1979) *Arch. Microbiol. 121*, 29−36.
11. Marrs, B. (1981) *J. Bacteriol. 146*, 1003−1012.
12. Prince, R. C., Stokley, K. E., Haith, C. A., and Jannasch, H. W. (1988) *Arch. Microbiol. 150*, 193−196.
13. Overmann, J., Beatty, J. T., Krouse, H. R., and Hall, K. J. (1996) *Limnol. Oceanog. 41*, 147−156.
14. George, M. J. (2000) *J. Synch. Rad. 7*, 283−286.
15. Sekiyama, H., Kosugi, N., Kuroda, H., and Ohta, T. (1986) *Bull. Chem. Soc. Jpn. 59*, 575−579.
16. (a) Jaklevic, J., Kirby, J. A., Klein, M. P., Robertson, A. S., Brown, G. S., and Eisenberger, P. (1977) *Solid State Commun. 23*, 679−682. (b) Waldo, G. S., Carlson, R. M. K., Moldowan, J. M., Peters, K. E., and Penner-Hahn, J. E. (1991) *Geochim. Cosmochim. Acta 55*, 801−814. (c) Tröger, L., Arvanitis, D., Baberschke, K., Michaelis, H., Grimm, U., and Zschech, E. (1992) *Phys. Rev. B 46*, 3283−3289. (d) Pfalzer, P., Urbach, J.-P., Klemm, M., Horn, S., denBoer, M. L., Frenkel, A. I., and Kirkland, J. P. (1999) *Phys. Rev. B 60*, 9335−9339.
17. McMaster, W. H., Kerr Del Grande, N., Mallet, J. H., and Hubell, J. H. *Compilation of X-ray Cross-Sections*, National Technical Information Service, Springfield.
18. http://www-ssrl.slac.stanford.edu/exafspak.html
19. George, G. N., Gorbaty, M. L., Kelemen, S. R., and Sansone, M. (1991) *Energy Fuels 5*, 93−97.
20. Guerrero, R., Mas, J., and Pedrós-Alió, C. (1984) *Arch. Microbiol. 137*, 350−356.
21. Greenwood, N. N., and Earnshaw, A. (1984) *Chemistry of the Elements*, pp 769−781, Pergamon Press, New York.

BI0105532